Flow Dynamics in a Triple Swirl Burner

Neha Vishnoi, Agustin Valera-Medina, Aditya Saurabh, and Lipika Kabiraj

Abstract One of the most important milestones in gas turbine burner technology was the incorporation of swirling flows for flame stabilization. The objective of present work is the design and development of a generic fuel flexible multiple swirl burner with enhanced flashback resistance and low emissions. The burner design will allow operation in premixed and non-premixed modes with liquid and gaseous fuels. The investigated burner consists of 3 annular co-rotating swirlers: an outer radial swirler stage and two concentric axial swirler stages. Insights from the first isothermal and reactive numerical simulations for premixed methane–air combustion are being presented here. Results based on the characterization of the flow fields, temperature distribution, streamwise and azimuthal shear layer dynamics, and turbulence characteristics are presented. The velocity profiles obtained from isothermal numerical simulations are also validated by experimental results. Flame stabilization and flashback propensity are discussed with respect to the features of vortex breakdown, specifically the central recirculation zone (CRZ).

Keywords Central recirculation zone · Fuel flexibility · Flashback · Swirl flow

1 Introduction

Incorporation of swirling flows for flame stabilization in gas turbines is a crucial milestone in the industry that allows for efficient, and stable combustion with low NOx emissions [17]. In such combustors, swirl is introduced to the incoming fuel–air mixture by stationary swirl vanes, which creates a vortex flow centered on the com-

N. Vishnoi (✉) · L. Kabiraj
Indian Institute of Technology Ropar, Rupnagar, Punjab, India
e-mail: 2018mez0019@iitrpr.ac.in

A. Valera-Medina
Cardiff University, Cardiff, Wales, UK

A. Saurabh
Indian Institute of Technology Kanpur, Kanpur, UP, India

G. Sivaramakrishna et al. (eds.), *Proceedings of the National Aerospace Propulsion Conference*, Lecture Notes in Mechanical Engineering,
https://doi.org/10.1007/978-981-19-2378-4_34

bustor's centerline. At significantly high swirl intensity, vortex breakdown occurs in the combustion chamber, thus forming recirculation zones. These recirculation zones mix hot products into reactants upstream of flame base. These recirculation zones are also responsible for increasing the flame speed [5]. At optimum swirl intensity, the flame is stabilized at the dump plane in the shear layers and is compact permitting the design of a shorter and lighter combustor. Additionally, swirl flows provide the control of the mixing pattern and temperature field for preventing autoignition, and flashback [10]. Vortex breakdown [6] is associated with formation of helical structures [23], and precessing vortex core (PVC) [1, 18] that acts as a source of unsteady flow and heat release, thus triggering thermoacoustic instabilities in the system. To address the stability issues associated with swirl flow, understanding the dynamics of vortex breakdown is crucial.

Most gas turbines are operated using natural gas because of its availability, low cost, and reliability. However, a combination of recent factors, including volatility in fuel supply and pricing, global and climatic concerns about carbon emissions, and excess risk from heavy dependence on a single energy source, have made the utilization of natural gas substitutes such as industrial, municipal, and agricultural opportunity fuel sources very attractive from environmental and economic standpoints. Nevertheless, a major barrier to the utilization of opportunity fuels remains in the inability of industrial gas turbines to operate effectively when powered by such fuels [26]. The lean premixed swirl stabilized combustors burning a wide variety of fuels are prone to flashback because they are highly tuned to operate on low-flame-speed fuels like natural gas. A solution to these hurdles is to develop state-of-the-art technologies for diluent-free ("dry") or wet, low NOx and flashback-resistant combustion for fuel flexible gas turbines [2]. Lately, the leading gas turbine manufacturers like GE, Siemens, Hitachi, and dedicated research groups are focused on developing such state-of the-art technologies [7]. The available fuels, being investigated, cover a wide range of Wobbe indices from those of high hydrogen content syngas produced in the IGCC with CO_2 capture and storage (CCS) systems to that of propane, and a wide range of flame speeds from that of natural gas to those of high hydrogen content fuels [2].

The long-term aim of the present work is the development of a novel fuel flexible multiple swirl burner with reduced detrimental thermoacoustic instabilities, low NOx emissions, and stable combustion. The fuel blends to be specifically tested are methane-hydrogen or pure hydrogen. Toward this, a preliminary design for burner is proposed and comparative study of flow fields for isothermal and reactive flows has been investigated through numerical simulations. Reynolds Averaged Navier-Stokes (RANS) [4] simulation approach has been utilized here for flow description. This approach with simplistic combustion models [4] helps in simulating the mean flow field and effects of entire range of turbulent scales. Observations from the first set of simulations are presented as a function of axial velocity contours, turbulent kinetic energy contours, axial and tangential velocity profiles, and temperature fields. Experimental validation of RANS isothermal flow profiles has also been conducted. Streamwise and azimuthal shear layers are characterized by vorticity contours and profiles.

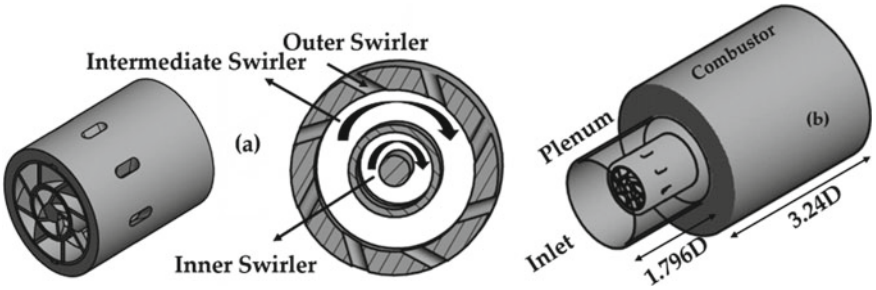

Fig. 1 **a** Triple swirl burner assembly and its perpendicular section; **b** computational domain

2 Test Case: Triple Swirl Burner

Triple Annular Research Swirler (TARS), a fuel injector, was developed by Goodrich Corporation in collaboration with General Electric Aircraft Engines (GEAE) for research purposes [21]. It has a complex geometry with design features analogous to an aero-engine application and has been investigated in numerous experimental and numerical studies [10, 16, 17]. A peculiar characteristic of TARS is the propagation of central recirculation zone (CRZ) upstream of the fuel injector exit, thereby stabilizing the flame inside the injector [8, 11]. The burner design investigated in the present work is derived from the TARS concept. The investigated burner is characterized by three co-axial air passages: outer radial swirlers and intermediate and inner axial swirlers (Fig. 1a). Different configurations of the burner can be realized by changing the swirl configuration (altering the vane angles of the three swirlers) or rotating direction (co-rotating or counter-rotating) to generate different swirling flow fields. In the present work, all the swirlers are co-rotating and the swirl configuration is $S504555$ corresponding outer, intermediate, and inner swirl vane angles of 50°, 45°, and 55°, respectively. The outer and intermediate swirlers comprise 8 vanes while the inner swirler has 5 vanes. The swirl numbers for the outer, intermediate, and inner swirlers are 0.79, 0.77, and 1.061, respectively. The overall length of the burner is 66 mm. The exit diameter of the burner is $D = 54$ mm and would be used as reference for normalizing coordinates.

3 Numerical Details: Computational Domain and Boundary Conditions

The dynamics of the flow within the triple swirl burner and in the combustor is simulated using RANS (Reynold's Averaged Navier-Stokes) numerical model in STAR CCM+ at GTRC (Gas turbine research center), Cardiff University. Owing to the complex geometry of the burner, an unstructured polyhedral mesh with prism layer composed of 8.05 million cells was generated. SST $k - \omega$ turbulence model was

Table 1 Operating conditions for triple swirl burner

Condition	Case 1		Case 2		Φ
	$\dot{m}_a$ (g/s)	$\dot{m}_f$ (g/s)	$\dot{m}_a$ (g/s)	$\dot{m}_f$ (g/s)	
Isothermal	8.73	–	19.25	–	–
Reactive	8.73	0.379	19.25	0.835	0.75

used to predict the burner's exit flow field. The turbulent flame closure combustion model used for simulations is Zimont's TFC model [27]. This model involves the solution of a transport equation for the reaction progress variable. The closure of this equation is based on the definition of the turbulent flame speed. For the resolution of combustion,"Complex Chemistry" was employed, enabling the calculation of molar and mass fractions, chemical rates of production and heat release with up to 130 reactions and 27 species. Simultaneously, clustering methods were employed to reduce the computational expense of these Complex Chemistry calculations. The computational domain is presented in Fig. 1b. It consists of a plenum—upstream the burner, the burner itself, and a cylindrical confinement. The inlet is located at about $1.796D$ upstream of the dump plane. The cylindrical confinement is $3.24D$ long and $2.85D$ in diameter.

At inlet, for pressure, zero gradient condition is imposed. For temperature and species mass fractions, Dirichlet conditions are imposed. The inlet air temperature is 300 K. At the outlet, pressure is atmospheric (101 kPa). No slip conditions are assumed at the walls with zero pressure gradient and species mass fractions. The walls are assumed to be adiabatic. The origin of the coordinates is placed near the center of the inlet of the plenum. The operating conditions for the present numerical study are tabulated in Table 1. Premixed air–fuel mixtures after passing through the triple swirl burner enter the dump combustor.

where $\dot{m}_a$ and $\dot{m}_f$ represent air and fuel (methane) flow rates, respectively. Φ represents equivalence ratio.

4 Laboratory Experiments

Isothermal experiments were performed using a vertical atmospheric test rig facility (Fig. 2) at Cardiff University. The test rig consists of a vertical air flow conditioning chamber, and a funnel extension for mounting of the burner. The experiments were performed for case 1 isothermal flow condition, and mean axial velocity data was obtained at different axial locations downstream the burner exit (Fig. 2) through LDA (Laser Doppler Anemometry) diagnostic technique.

A 3D Dantec traverse system, controlled by BSA software, was used to move the laser head stably in horizontal and vertical directions relative to the test rig. For experiments, the triple swirl burner with plenum was 3D printed using Polyamide

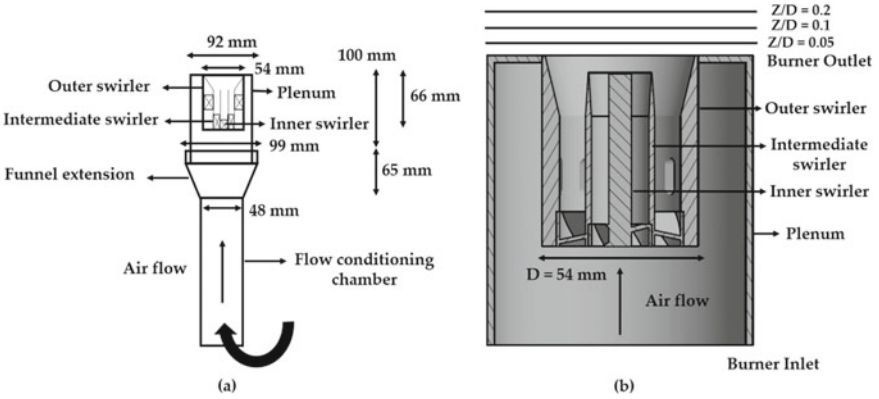

Fig. 2 Schematic of vertical atmospheric test rig and cross-section of burner with experimental measurement points

(Nylon (PA2200)) material. This material has good mechanical properties, dimensional stability, wear resistance, and high chemical resistance [14]. The air flow rate of 440 ltr/min was metered by Platon flow meter at a constant pressure of 2 bars. Aluminum dioxide powder was used as the seeding particles for flow visualization.

5 Results and Discussions

Formation of CRZ with reversed flow at burner's axis because of vortex breakdown is the characteristic feature of swirling [3]. The shape and location of formation of CRZ is a function of swirl intensity and inlet Reynold's number [17]. These flows are 3-dimensional whose dynamics are dependent on geometric considerations. In the present study, comparative flow fields from isothermal and premixed methane–air reactive simulations are presented and are characterized as a function of axial velocity streamwise and cross stream contours, turbulent kinetic energy contours, axial and tangential velocity profiles, and temperature fields. The information about the formation of inner and outer shear layers is provided through vorticity contours and profiles.

5.1 Velocity Field

Figures. 3 and 4 shows the streamwise axial velocity contours for flow field along the central axis of the burner for cases 1 and 2, respectively. A swirling motion is imparted to the air when passing through the three set of vanes which along with their shear layers merges near the burner exit. From the flow fields inside the burner

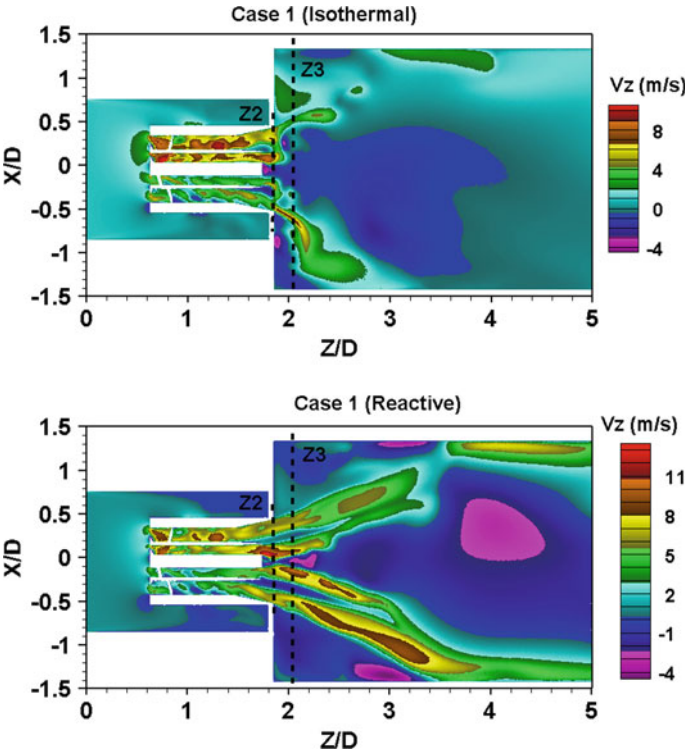

Fig. 3 Comparison of streamwise isothermal and reactive flow axial velocity contour for case 1. The coordinates are normalized by $D = 54\,\text{mm}$

and plenum assembly, for all conditions, regions of reversed flow can be observed at the solid surface of outer swirler and plenum body (indicated by blue color for case 1 and blue and dark cyan colors for case 2). The highest velocities are observed throughout the flow passages in the burner.

Regions of reversed flow are observed at the tips of intermediate and inner swirlers which favors the merging of the jets. Unlike TARS, the inner swirler rod is extended up to the exit; therefore, no upstream propagation of CRZ through central route is possible. The reverse flow at the tips of inner swirler merges with the CRZ. Along the walls of the burner, boundary layer detachment is also observed. These observations are crucial for burner design in terms of two types of flashback [24]: boundary layer flashback when flame gets attached to burner rim and flashback due to upstream propagation of CRZ. In the present case, for the mass flow rates considered, flashback through inner and intermediate swirler tips is possible. This is the point of consideration for further modification in the burner design especially for incorporation of highly reactive fuels.

From the isothermal fields inside the combustor, the shape and size of CRZ can be comprehended. The shape of CRZ is spherical (approximately) as represented

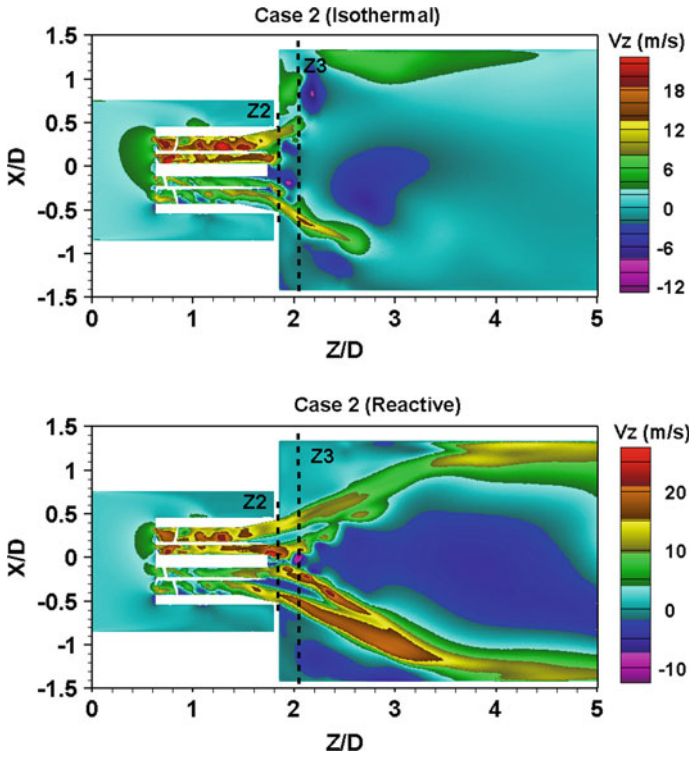

Fig. 4 Comparison of streamwise isothermal and reactive flow axial velocity contour for case 2. The coordinates are normalized by $D = 54\,\text{mm}$

by blue color. The width of CRZ is $\pm 0.2D$ at the burner exit ($Z/D = 1.84$) which increases up to $\pm 0.75D$ at $Z/D = 3.5$. It is necessary to note these observations for size and strength of CRZ. Addition of highly reactive fuels like hydrogen to methane causes the upward shifting of the CRZ and also affects its size and strength which forms the basis for flashback [13]. Outside the CRZ, an annular jet emerges from the burner as indicated by green, yellow, and orange colors.

Changes in the temperature and density as a result of combustion heat release causes changes in the velocity flow fields when compared to isothermal conditions. For the reactive fields, the CRZs are strong for both the cases and differ in size and location relative to the burner exit when compared to isothermal cases. For the reactive cases, the CRZ is lifted and is narrowed near the burner exit. Its size becomes remarkably smaller, only $\pm 0.05D$ compared to $\pm 0.2D$ for the isothermal case at the exit. Further downstream, its size reduces. The CRZ is pushed downstream in the combustor with higher flow rates as can be seen for case 2. This reduces the chances of its upstream propagation through intermediate and inner swirler tips.

Figure 5 represents the velocity distribution at the exit plane of the burner (marked as Z2 in Figs. 3 and 4). The distribution shows the presence of CRZ with negative axial

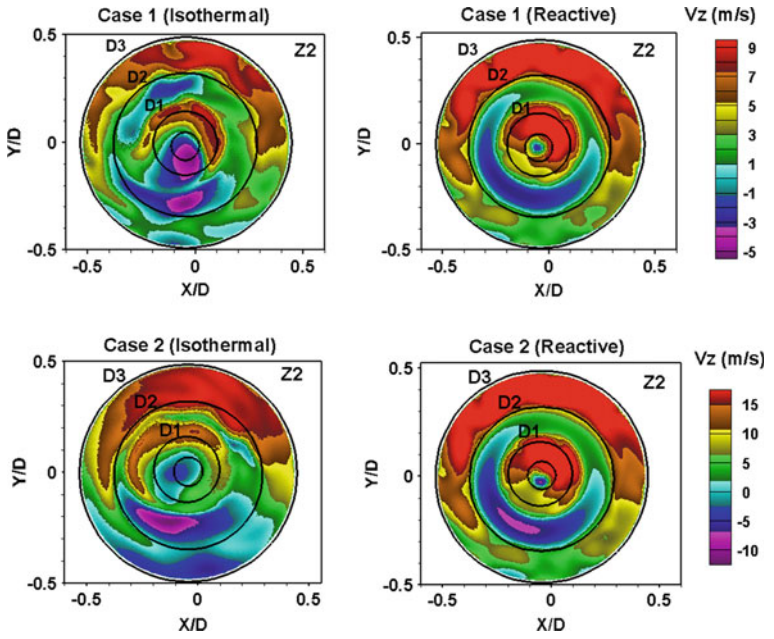

Fig. 5 Comparison of crosswise axial velocity contours at the exit of the burner (plane Z2) for isothermal and reactive flows. The coordinates are normalized by $D = 54\,\text{mm}$

velocity around the axis of the burner. The strength of CRZ is low for reactive cases at burner exit confirming the lifting and constriction of CRZ in reactive flows. The non-uniformity of velocity distribution at the burner axis is captured by these contours. 2–4 velocity peaks can be observed at the burner exit. These peaks can be associated with the vane angles and number of vanes [8]. The flow generated by the swirlers was not completely mixed at the exit resulting in non-uniform flow with velocity values higher at certain regions. Such non-uniformities were also reported for TARS in various numerical and experimental studies [8, 10, 12]. For both isothermal and reactive flows, the reverse velocity regions at swirler tips (D1 and D2) are pronounced indicating the presence of a possible route to flashback and flame anchoring location. Improvements in the burner design need to be made for mitigating this flashback route.

The turbulent kinetic energy contours are representatives of the distribution of total turbulence from burner exit. Figure 6 represents the comparison of these contours for isothermal and reactive cases. From isothermal cases, it can be observed that the turbulence is robust at inner shear layer between annular jet and CRZ, whereas it is lowest inside CRZ. This intensity in the shear layer is nearly twice the level in CRZ for both the cases. This result agrees with the TARS configuration [17].

Combustion affects the distribution of turbulent kinetic energy by clearly defining the low- and high-turbulence velocity regions (Fig. 6) and disperses the turbulence

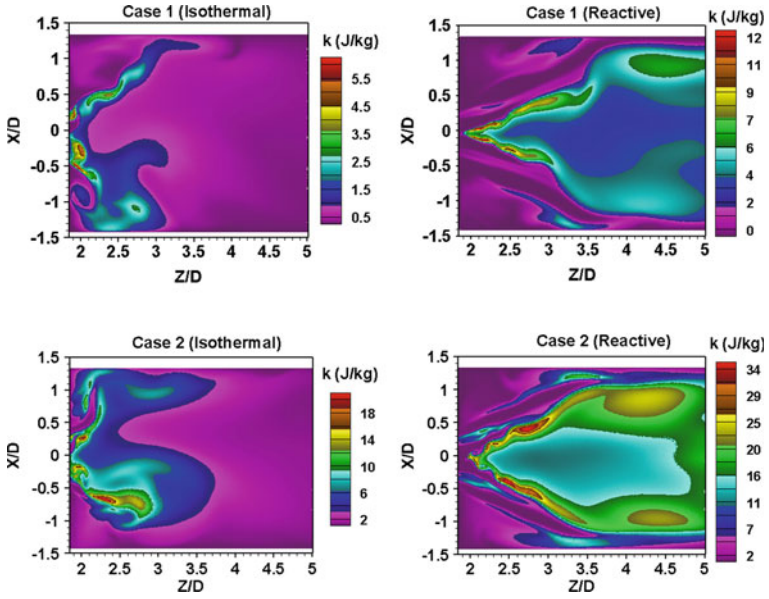

Fig. 6 Comparison of turbulent kinetic energy contours for isothermal and reactive flows inside the combustor

field into patches of turbulent regions. Like isothermal flows, the annular jet has higher turbulence compared to the inside of CRZ. Similar effect of combustion on turbulence is observed in TARS [17].

To quantify the observations from the velocity contours, spatially averaged axial and tangential velocity profiles are plotted for isothermal and reactive flows and are presented in Fig. 7. These profiles are obtained at Z2 and Z3 planes as marked in Figs. 3 and 4. Since, mass flow rates are not constant for the cases considered, all the velocity values have been normalized by $V_0 = 7.1 m/s$ (case 2) for comparison purposes.

As observed from crosswise contours, the velocity distribution has 4 peaks along the burner diameter and reversed flow at the swirler tips (D1 and D2 in isothermal and D2 in reactive flows, respectively) are also visible. These peaks are defined in Fig. 7. For reactive flows, positive velocity peaks are observed at the center of the burner unlike isothermal profiles even though the mass flow rates are constant for a particular case. The reason for this trend of velocity profiles can be explained by the temperature contours (Fig. 9). For reactive flows, the flame is found to flashback through the inner and intermediate swirler passages and is anchored inside the burner. Due to higher temperature regions at the tips of swirlers, the density reduces resulting in the increase in velocity and mass flow rates. The radial motion of the swirling flow is also observed to be enhanced remarkably by combustion (as observed from tangential profiles—red and green markers). Although the boundary conditions are

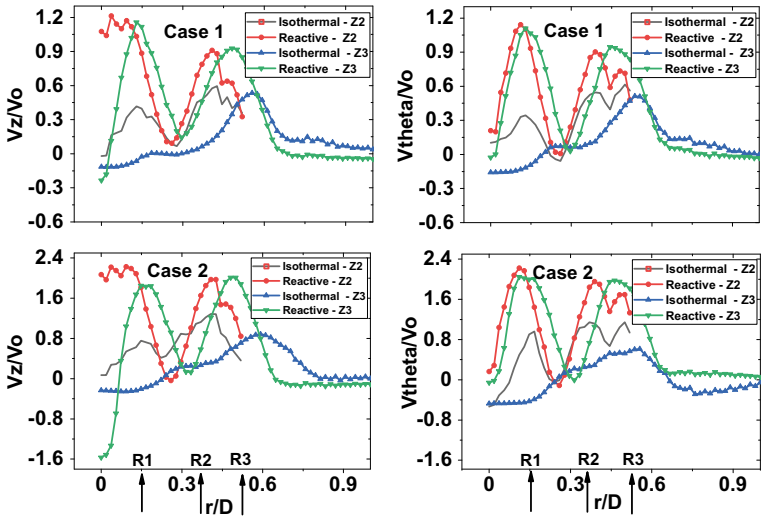

Fig. 7 Comparison of radial profiles of axial (left) and tangential velocities (right) for isothermal and reactive flows. Z2 and Z3 are the planes at burner exit and, in the combustor, respectively, as marked in Figs. 3 and 4. The velocity values are normalized by V_0

symmetric, yet flow fields are found to be non-uniform. These non-uniformities are typical for this design and are not observed in TARS.

5.2 *Experimental Validation of Velocity Field*

Figure 8 presents the comparison of mean axial velocity profiles obtained from RANS simulations and experiments at $Z/D = 0.05, 0.1,$ and 0.2 downstream the burner exit (consider the coordinates to be placed at the center of the burner exit). The plots characterize the non-uniform features of the flow field. The axial velocity mapping indicates a CRZ with reverse velocity. The width of CRZ increases on moving in downstream direction. Velocity profiles obtained from RANS simulations matches with the experimental profiles except for the location of peak velocity.

The velocity distribution from RANS simulations indicates the presence of separated flow at the boundaries of the swirlers (D1 and D2). This flow separation leads to the inward shifting of annular jet resulting in velocity displacement. However, no such flow separations are observed in experimental results (Fig. 8) indicating the attached flow. This disagreement between the RANS simulations and experimental results suggests the incapability of RANS to predict accurate behavior of turbulent swirling flow near a diverging region. Therefore, the next step would be to use the data obtained from experiments as inlet boundary conditions numerical model validation using LES.

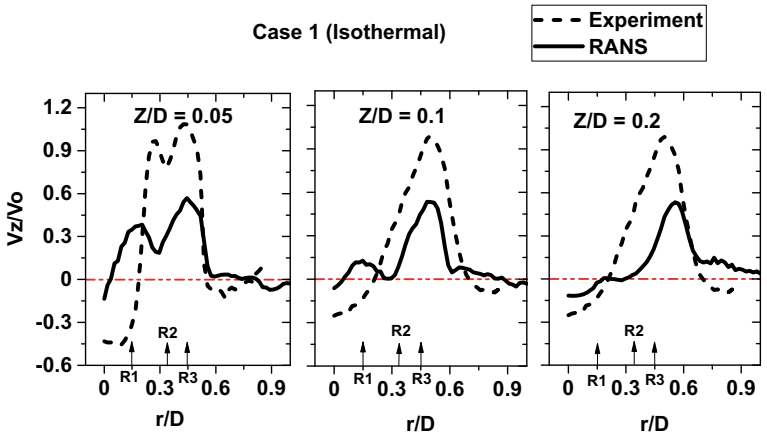

Fig. 8 Comparison between isothermal experiments and RANS simulation results for axial velocity profiles for Case 1 at different axial locations in the combustor. The coordinates are normalized by $D = 54\,\text{mm}$ and velocity value by V_0

5.3 Temperature Distribution

Figure 9 shows the temperature distribution for reactive case 1 and 2 in the combustor. The temperature is uniformly distributed inside the combustor on both the sides of the burner axis and peak temperatures of around 2300 K and 1900 K are observed for the two cases, respectively. From the contours, it is observed that the flame is flashing back through the tips of inner and intermediate swirlers. The flame is stabilized at the inner shear layer between the swirling jet and CRZ, and at outer shear layer with the surrounding air and is anchored inside the burner. We are using adiabatic conditions for simulations therefore the difference in peak temperatures is possible. In practice, most burners would operate in the range of $\Phi = 0.6 - 0.65$ to bring down those temperatures, besides they would operate with an increase in pressure that would also reduce the flame size, thus controlling turbulence and mitigating large temperature spots. Therefore, we require some experiments for calibration of the model, including some temperature profiles of the casing/burner to determine heat transfer and more realistic values. This will be assessed through experimentations in further work. The temperature drops in the shear layers as can be visualized from radial profiles. Beyond the burner radii, the temperature field is constant and is toward the lower side. These observations from the contours suggest that the present configuration requires design modifications in terms of swirl number and Reynold's number. The higher flow rates may help in reducing the flashback issue but this may not help with higher reactive fuels.

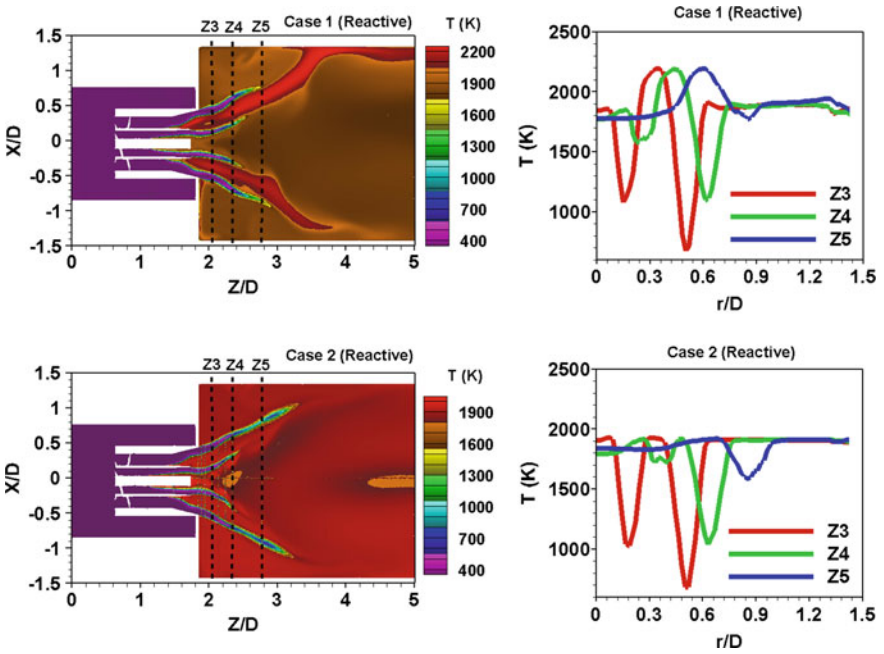

Fig. 9 Comparison of temperature distribution and its averaged radial profiles for reactive flow cases 1 and 2. The coordinates are normalized by $D = 54\,\text{mm}$

5.4 NOx Emission Profiles

The methodology to determine NOx (NO, NO_2, etc.) was through the resolution of the complex chemistry, thermodynamics, and transport properties of the complex mechanism. Figure 10 represents the radial profile of NO2 emissions for the reactive flow case 2 at two axial locations farther downstream the burner exit. As the peak temperatures for case 2 lies within the range of 1800–1900 K, at an equivalence ratio of 0.75, the emission range is as expected, i.e., up to 4 ppm [20]. The emissions are higher near the burner center and reduce toward the walls of the combustor. NO2 emissions increase exponentially with flame temperature. The contours for NOx emission suggest that the emissions are within the reasonable range for lean premixed mixtures.

5.5 Shear Layer Dynamics

Figure 11 shows the characteristic features of a swirling jet. These features include an annular jet that emanates from the nozzle exit and passes between recirculation zones (inner (IRZ) and outer (ORZ)). The IRZ is associated with the interactions between

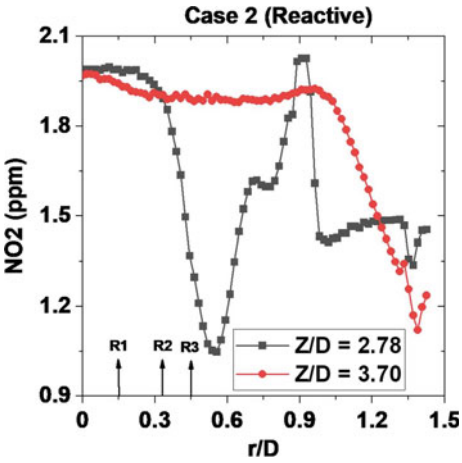

Fig. 10 Comparison of radial profiles of NO2 emissions for reactive case 2 at two axial locations in the combustor: $Z/D = 2.78(Z5)$ and $Z/D = 3.70$

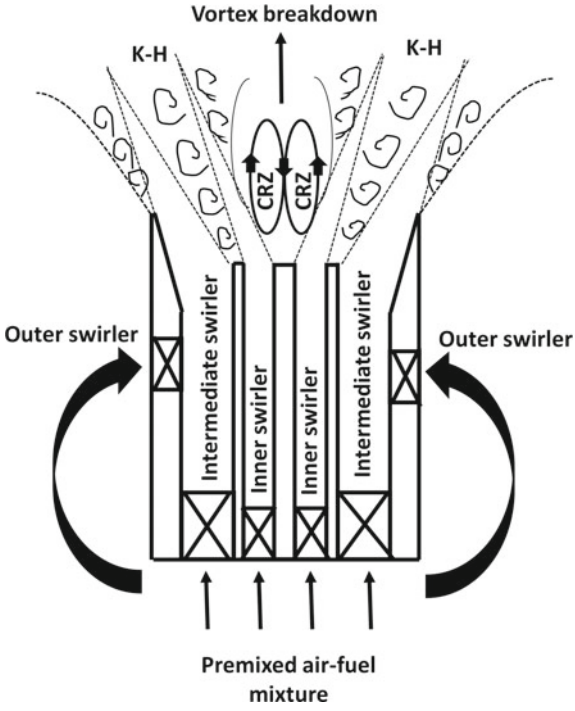

Fig. 11 Schematic representing features of a swirling jet. K-H indicate Kelvin–Helmholtz instability. This figure is reproduced from O'Conner et al. (2011) for triple swirl burner

vortex breakdown bubble (VBB) and center-body wake. This flow field forms the base flow in which the perturbations can grow or decay. Leibovich [15] and Rusak and Wang [22] presents an extensive study on VBB and instabilities. The size and location of VB is dependent on the swirl intensity, axial pressure gradient, geometrical features, and Reynold's number [19]. Streamwise and spanwise shear layers separates

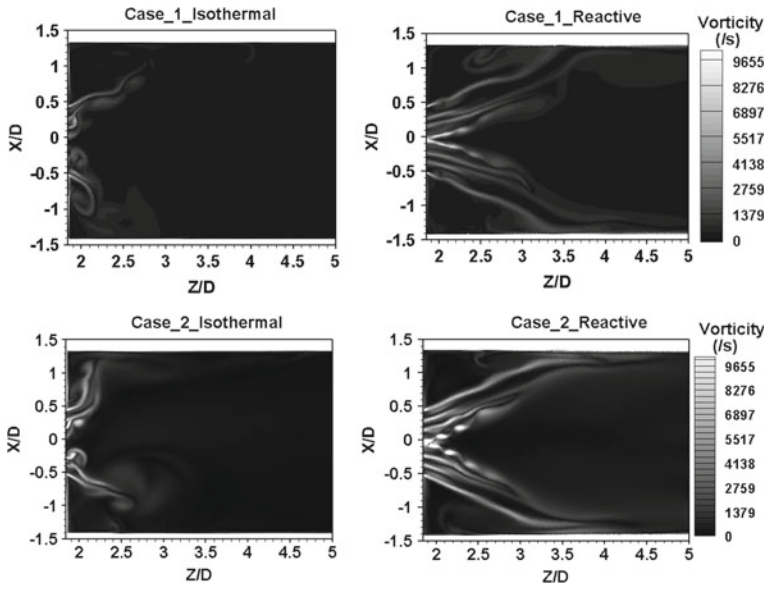

Fig. 12 Comparison of streamwise vorticity contours for shear layer visualization between isothermal and reactive flows. The coordinates are normalized by $D = 54\,\text{mm}$

the annular jets and RZ. The shear layers are unstable and are associated with vortex rollup and forms concentrated regions of vorticity [9]. The flame is stabilized at inner shear layer between annular jet and CRZ and at the outer shear layer separating ORZ.

In the present study, the shear layer dynamics is presented by plotting the streamwise vorticity contours for isothermal and reactive flows. Figure 12 represents the comparison for the contours. The wrinkling of the shear layers is associated with vortex roll up that are convected in the downstream direction. Figure 12 clearly represents the vortex rollup phenomena. The beginning of the vortex rollup in inner shear layer (ISL-between CRZ and swirling jet) is clearly visible in the figure. These vortices grow as they convect downstream. These vortices are larger in size due to their interactions with CRZ. The presence of additional shear layers between inner and outer layers are indicative of multiple swirl passages in the burner.

Figure 13 shows the azimuthal shear layer through cross stream vorticity contours at two axial locations inside the combustor: $Z/D = 1.94$ and $Z/D = 2.04$ for reactive flows. The inner and outer shear layers along with two additional shear layers are clearly demarcated. These additional shear layers are generated due to multiple swirl passages and boundaries in the burner. The structures in these layers are larger in size and can be seen to roll up as the flow rotates. Due to the interaction of ISL with CRZ, the vortical structures in ISL are large and more diffuse. Figure 14 represents the vorticity profiles for the reactive cases along the line marked on Fig. 13. The presence of large vortical structures can be clearly seen in ISL with high magnitude of vorticity.

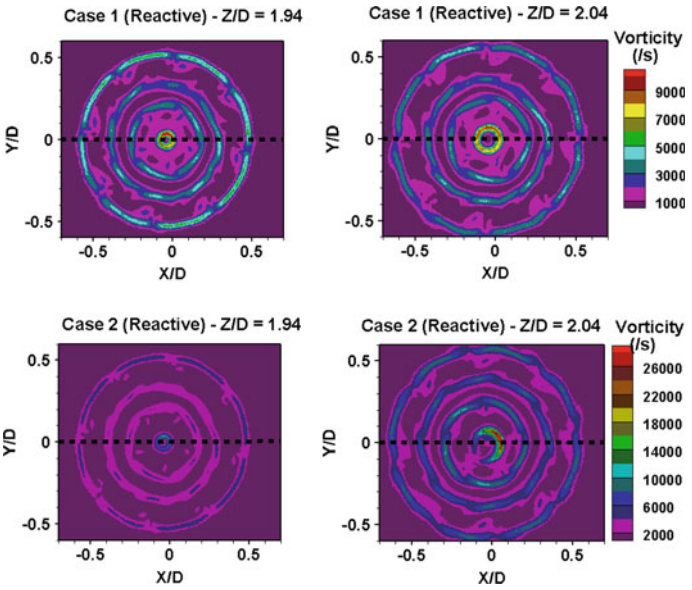

Fig. 13 Cross wise vorticity contours at two axial locations in the combustor: $Z/D = 1.94$ and $Z/D = 2.04$. The coordinates are normalized by $D = 54\,\text{mm}$

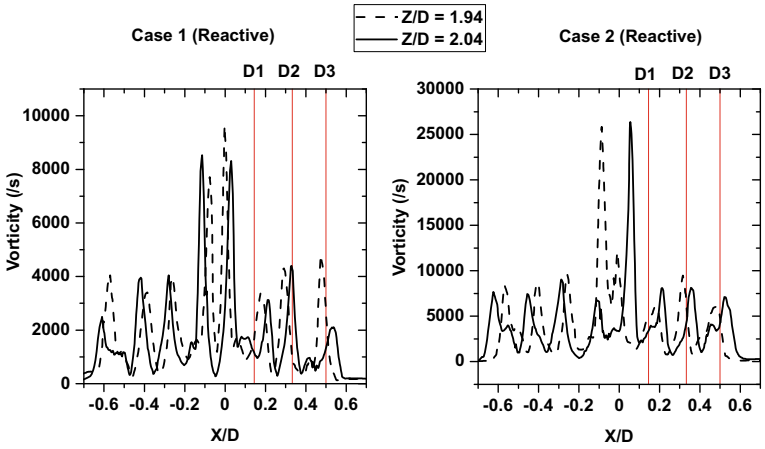

Fig. 14 Vorticity profiles for reactive flows at the locations marked in Fig. 13. The coordinates are normalized by $D = 54\,\text{mm}$

Thumuluru and Lieuwen [25] have experimentally reported four flame topologies based on the position of VBB. The flame is anchored at the stagnation point behind the VBB, if it is detached from the center body. On the contrary, if the VBB is attached to the center body, the flame is stabilized in one or both the shear layers.

In the present configuration, VBB is attached to the inner swirler body, and flame is stabilized in the ISL. The flame has a tendency to stabilize on the intermediate swirler rim, thus creating an adverse effect on burner body. Higher flow rates and modifications in the burner are required to increase the Reynolds number.

6 Concluding Remarks

The abovementioned behavior of swirlers highlights the importance of parameters that govern these flows: swirl numbers, number of swirl vanes, the inlet boundary conditions, velocity profiles, and shear layer dynamics. Swirl of sufficient strength induces an adverse pressure gradient which causes vortex breakdown and flow reversal. This work aims at developing a generic fuel flexible swirl burner which can be operated in premixed or non-premixed modes and have stable combustion with minimum flashback. Toward this aim, a preliminary design of the burner employing three swirlers was proposed and corresponding mean flow fields were investigated with the help of RANS simulations. Compared to the top-hat velocity profiles, the triple swirl burner's profiles involve complex features. The isothermal and reactive flow fields indicate the upward propagation of recirculation zones causing the flame to stabilize inside the burner. This upstream propagation is not as severe as that of TARS but is a crucial consideration especially when dealing with higher reactive fuels. Higher temperature ranges are observed which may lead to higher NOx emissions but as the present cases are simulated for adiabatic conditions, practical assessment of the burner will help in estimating the actual temperatures. The RANS simulation results are also validated using initial isothermal experiments, and the results were found to be well in agreement.

The ongoing work address appropriate methods to improve the flow fields. The issues to be explained relate to mitigating any chances of flashback, incorporating liquid and gaseous fuels injection locations, and using suitable laboratory data for LES simulations.

Acknowledgements This work is funded by SPARC project (No: SPARC/2018-2019/P243/SL) sponsored by MHRD. The simulations and experimental investigations were conducted at GTRC, Cardiff University.

References

1. Anacleto P, Fernandes E, Heitor M, Shtork S (2003) Swirl flow structure and flame characteristics in a model lean premixed combustor. Combustion Sci Technol 175(8):1369–1388
2. Asai T, Miura K, Akiyama Y, Karishuku M, Yunoki K, Dodo S, Horii N et al (2016) Development of fuel-flexible gas turbine combustor. In: Proceedings of the 45th turbomachinery symposium, Turbomachinery Laboratories, Texas A&M Engineering Experiment Station
3. Beér JM (1974) Combustion aerodynamics. In: Combustion technology. Elsevier, pp 61–89

4. Bray K (1996) The challenge of turbulent combustion. In: Symposium (international) on combustion, vol 26. Elsevier, pp 1–26
5. Driscoll J, Temme J (2011) Role of swirl in flame stabilization. In: 49th AIAA aerospace sciences meeting including the New Horizons forum and aerospace exposition, 108
6. Duwig C, Fuchs L, Lacarelle A, Beutke M, Paschereit CO (2007) Study of the vortex breakdown in a conical swirler using ldv, les and pod. Turbo Expo: Power Land Sea Air 47918:1–10
7. Global E (2020) Hydrogen gas turbines: the path towards a zero-carbon gas turbine. ETN Global 2
8. Grinstein FF, Young TR, Gutmark EJ, Li G, Hsiao G, Mongia HC (2002) Flow dynamics in a swirl combustor. J Turbulence 3(1):030
9. Ho CM, Huang LS (1982) Subharmonics and vortex merging in mixing layers. J Fluid Mech 119:443–473
10. Iudiciani P (2012) Swirl stabilized premixed flame analysis using of LES and POD. Lund University
11. Iudiciani P, Duwig C, Szász RZ, Fuchs L, Gutmark E (2011) Les of the interaction between a premixed flame and complex turbulent swirling flow. J Phys: Conf Ser 318:092007 (IOP Publishing)
12. Iudiciani P, Hosseini SM, Zoltan-Szasz R, Duwig C, Fuchs L, Collin R, Lantz A, Alde' n M, Gutmark E (2009) Characterization of a multi-swirler fuel injector using simultaneous laser based planar measurements of reaction zone, flow field, and fuel distribution. In: Turbo expo: power for land, sea, and air, vol 48838, pp 1041–1052
13. Kim HS, Arghode VK, Linck MB, Gupta AK (2009) Hydrogen addition effects in a confined swirl-stabilized methane-air flame. Int J Hydrogen Energy 34(2):1054–1062
14. Kundera C, Kozior T (2018) Mechanical properties of models prepared by sls technology. In: AIP conference proceedings, vol 2017. AIP Publishing LLC, 020012
15. Leibovich S (1978) The structure of vortex breakdown. Ann Rev Fluid Mech 10(1):221–246
16. Li G, Gutmark EJ (2005) Effect of exhaust nozzle geometry on combustor flow field and combustion characteristics. Proc Combustion Inst 30(2):2893–2901
17. Li G, Gutmark EJ (2006) Boundary conditions effects on nonreacting and reacting flows in a multiswirl combustor. AIAA J 44(3):444–456
18. Martinelli F, Olivani A, Coghe A (2007) Experimental analysis of the processing vortex core in a free swirling jet. Exp Fluids 42(6):827–839
19. OConnor J, Lieuwen T, Kolb M (2011) Visualization of shear layer dynamics in a transversely excited, annular premixing nozzle. In: 49th AIAA aerospace sciences meeting including the New Horizons forum and aerospace exposition, 237
20. Ouali S, Bentebbiche A, Belmrabet T (2016) Numerical simulation of swirl and methane equivalence ratio effects on premixed turbulent flames and nox apparitions. J Appl Fluid Mech 9(2)
21. Pritchard Jr BA, Danis AM, Foust MJ, Durbin MD, Mongia HC (2002) Multiple annular combustion chamber swirler having atomizing pilot. US Patent 6,381,964
22. Rusak Z, Wang S (1996) Review of theoretical approaches to the vortex breakdown phenomenon. In: Theoretical fluid mechanics conference, 2126
23. Shtork S, Vieira N, Fernandes E (2008) On the identification of helical instabilities in a reacting swirling flow. Fuel 87(10–11):2314–2321
24. Syred N, Giles A, Lewis J, Abdulsada M, Medina AV, Marsh R, Bowen PJ, Griffiths AJ (2014) Effect of inlet and outlet configurations on blow-off and flashback with premixed combustion for methane and a high hydrogen content fuel in a generic swirl burner. Appl Energy 116:288–296
25. Thumuluru SK, Lieuwen T (2009) Characterization of acoustically forced swirl flame dynamics. Proc Combustion Inst 32(2):2893–2900
26. Venkatesan K (2011) Fuel flexible combustion systems for high-efficiency utilization of opportunity fuels in gas turbines. Technical report, General Electric Company, Boston, MA (United States)
27. Zimont VL (2000) Gas premixed combustion at high turbulence. turbulent flame closure combustion model. Exp Thermal Fluid Sci 21(1–3):179–186